PERGAMON

Computers and Structures 79 (2001) 1839–1850

Computers & Structures

www.elsevier.com/locate/compstruc

Optimality criteria method for topology optimization under multiple constraints

Luzhong Yin, Wei Yang *

FML, Department of Engineering Mechanics, Tsinghua University, Beijing 100084, China

Received 15 August 2000; accepted 17 July 2001

Abstract

The existing framework of optimality criteria method is limited to the optimization of a simple energy functional with a single constraint on material resource. The present work extends the optimality criteria method to the case of multiple constraints. The difficulty in updating the Lagrangian multipliers is treated by gradient-split Taylor series expansion. Applications of the method are illustrated by computing the optimal structures under multiple displacement constraints, and by designing the material cells under given macroscopic elastic tensors that correspond to both positive and negative Poisson's ratios.

Keywords: Multiple constraints; Topology optimization; Optimality criteria; Optimal structures; Crack opening; Material design

1. Introduction

Structural topology optimization received considerable attention in recent years. Several approaches based on a density-like function were proposed [1,2], but resulted in optimization models with rather large number of design variables. Non-linear mathematical programming for such problems, on the other hand, is costly and time consuming. An attractive alternative is the *optimality criteria method*, which solves the optimality conditions directly if closed-form expressions can be derived [3]. The existing framework of optimality criteria method, however, is limited to the optimization of a simple energy functional (compliance [4] or eigenfrequencies) with a single constraint on material resource, as pointed out in the Refs. [2,5,6].

The present paper extends the optimality criteria method to problems with multiple constraints, and provides a generalized way to extract the optimality criteria. In the same spirit, the optimality criteria for tunnel support [7] and compliant mechanism [8] were established and solved.

Two types of problems exist in the literatures on topology optimization. One is to minimize a performance function, subject to equilibrium equations and the constraint on material resource. The other is to minimize the material resource, subject to equilibrium equations, and performance functions. The present work will focus on the second type of problems, namely to minimize the material volume under multiple displacement constraints.

2. Optimality criteria under multiple constraints

The problem of topology optimization under multiple constraints can be stated as follows:

$$\min\left(\phi = \int_{\Omega} \rho(\mu)\,\mathrm{d}\Omega\right), \tag{1}$$

such that

$$\int_{\Omega} \mathbf{u}\nabla : \mathbf{E}(\mu) : \mathbf{v}\nabla\,\mathrm{d}\Omega = \int_{\Gamma_t} \mathbf{t}\cdot\mathbf{v}\,\mathrm{d}\Gamma, \tag{2}$$

* Corresponding author. Tel.: +86-10-62782642; fax: +86-10-62781824.

E-mail address: yw-dem@tsinghua.edu.cn (W. Yang).

0045-7949/01/$ - see front matter
PII: S0045-7949(01)00126-2

$$\int_{\Gamma_t} h_\alpha(\mathbf{u})\,d\Gamma - \overline{h}_\alpha \leqslant 0, \quad \alpha = 1,\ldots,m, \tag{3}$$

$$\mu_{\min} \leqslant \mu \leqslant \mu_{\max}, \tag{4}$$

where μ denotes a design variable with the lower bound $\mu_{\min}$ and the upper bound $\mu_{\max}$, $\rho(\mu)$ the local density of the material, $\mathbf{E}(\mu)$ the material stiffness, Ω the design domain, Γ_t the traction boundary, $\mathbf{t}$ the traction acting on the structure, $\mathbf{u}$ and $\mathbf{v}$ the actual and the kinematically admissible displacements of the structure, h_α a pointwise function and $\overline{h}_\alpha$ the imposed value for the αth constraint, and m the total number of the displacement constraints.

The Lagrangian of the stated problem can be written as

$$\begin{aligned} L = &\int_\Omega \rho(\mu)\,d\Omega + \int_\Omega \mathbf{u}\nabla : \mathbf{E}(\mu) : \mathbf{v}\nabla\,d\Omega - \int_{\Gamma_t} \mathbf{t}\cdot\mathbf{v}\,d\Gamma \\ &+ \varphi_\alpha\left(\int_{\Gamma_t} h_\alpha(\mathbf{u})\,d\Gamma - \overline{h}_\alpha\right) + \int_\Omega z^-(\mu_{\min}-\mu)\,d\Omega \\ &+ \int_\Omega z^+(\mu-\mu_{\max})\,d\Omega\ , \end{aligned} \tag{5}$$

where φ_α $(\alpha = 1,\ldots,m)$ are the Lagrange multipliers for the displacement constraints; z^- and z^+ are the lower and upper bounds of material density. Summation convention implies for repeated indices unless specified otherwise. To cast all terms in the Lagrangian in the same physical dimension, $\mathbf{v}$, φ_α, z^- and z^+ are now regarded as normalized by a reference energy density. Stationary of the Lagrangian leads to the following Kuhn–Tucker conditions. For example, stationary with respect to the design variable μ implies:

$$\frac{\partial\rho}{\partial\mu} + \mathbf{u}\nabla : \frac{\partial\mathbf{E}}{\partial\mu} : \mathbf{v}\nabla - z^- + z^+ = 0, \tag{6}$$

and stationary with respect to the displacement $\mathbf{u}$ gives

$$\begin{aligned} &\Omega: \ (\mathbf{v}\nabla : \mathbf{E})\cdot\nabla = 0, \\ &\Gamma_t: \ \mathbf{v}\nabla : \mathbf{E}\cdot\mathbf{n} = -\varphi_\alpha\frac{\partial h_\alpha}{\partial\mathbf{u}}. \end{aligned} \tag{7}$$

The linearity with respect to the kinematically admissible displacement $\mathbf{v}$ admits a solution of superposition type:

$$\mathbf{v} = -\varphi_\alpha\mathbf{v}_\alpha, \tag{8}$$

where $\mathbf{v}_\alpha$ is the auxiliary field for the αth constraint:

$$\begin{aligned} &\Omega: \ (\mathbf{v}_\alpha\nabla : \mathbf{E})\cdot\nabla = 0, \\ &\Gamma_t: \ \mathbf{v}_\alpha\nabla : \mathbf{E}\cdot\mathbf{n} = \frac{\partial h_\alpha}{\partial\mathbf{u}} \quad (\alpha = 1,\ldots,m). \end{aligned} \tag{9}$$

They assemble the equilibrium equations and the traction boundary conditions of the adjoint structures [10], and consequently can be solved together with the structural equilibrium equations, without substantial increase in computer time.

Substituting Eq. (8) into Eq. (6), one has

$$\frac{\partial\rho}{\partial\mu} - \varphi_\alpha\mathbf{u}\nabla : \frac{\partial\mathbf{E}}{\partial\mu} : \mathbf{v}_\alpha\nabla - z^- + z^+ = 0. \tag{10}$$

The Lagrange multipliers φ_α $(\alpha = 1,\ldots,m)$ can be updated by the constraint equation (3). A relation between the constraint and the design variable can be revealed by Taylor series expansion of Eq. (3) near a known point $(\mu_0, \mathbf{u}_0)$:

$$\begin{aligned} &\int_{\Gamma_t} h_\alpha(\mathbf{u}_0)\,d\Gamma + \int_\Omega \mathbf{u}\nabla : \mathbf{E}(\mu) : \mathbf{v}_\alpha\nabla\,d\Omega \\ &\quad - \int_\Omega \mathbf{u}_0\nabla : \mathbf{E}(\mu_0) : \mathbf{v}_{\alpha 0}\nabla\,d\Omega \leqslant \overline{h}_\alpha, \end{aligned} \tag{11}$$

where $\mathbf{v}_{\alpha 0}$ is the known values of $\mathbf{v}_\alpha$ at the given point $(\mu_0, \mathbf{u}_0)$. During the Taylor series expansion, the gradient of $\mathbf{u}$ near $\mathbf{u}_0$ is split into $\mathbf{u}\nabla$ in the second term and $\mathbf{u}_0\nabla$ in the third term of Eq. (11) to facilitate the iteration. Eq. (11) provides an implicit relation between $\mathbf{u}$ and $\mathbf{E}$. Adopting the fixed-point update scheme, one only updates μ and leaves $\mathbf{u}$ unchanged. When the structure is loaded by displacement constraint, one can use Eq. (11) to update the Lagrange multipliers, as will be exemplified in Section 4.

For traction-loaded structures, one should transform Eq. (11) into the stress form

$$\begin{aligned} &\int_{\Gamma_t} h_\alpha(\mathbf{u}_0)\,d\Gamma + \int_\Omega \sigma : \mathbf{C}(\mu) : \sigma_\alpha\,d\Omega \\ &\quad - \int_\Omega \mathbf{u}_0\nabla : \mathbf{E}(\mu_0) : \mathbf{v}_{\alpha 0}\nabla\,d\Omega \leqslant \overline{h}_\alpha, \end{aligned} \tag{12}$$

where $\mathbf{C}$ denotes the structure compliance, σ the stress tensor, and σ_α the stress tensor of the adjoint structure. Examples of such optimization problems will be presented in Section 3. Eqs. (10) and (11) or Eq. (12) give rise of an iteration scheme for optimality criteria.

Consider the special case that $h_\alpha(\mathbf{u})$ is a homogeneous function of $\mathbf{u}$ of degree n. The Euler's theorem states that:

$$h_\alpha = \frac{1}{n}\mathbf{u}\cdot\frac{\partial h_\alpha}{\partial\mathbf{u}}. \tag{13}$$

By the principle of visual work, the integral form of the above expression can be phrased as:

$$\int_{\Gamma_t} h_\alpha\,d\Gamma = \frac{1}{n}\int \mathbf{u}\nabla : \mathbf{E} : \mathbf{v}_\alpha\nabla\,d\Omega. \tag{14}$$

The same expression holds true at point $\mathbf{u}_0$. Accordingly, Eqs. (11) and (12) can be simplified to:

$$\int_\Omega \mathbf{u}\nabla : \mathbf{E} : \mathbf{v}_\alpha\nabla\,d\Omega - (n-1)\int_{\Gamma_t} h_\alpha(\mathbf{u}_0)\,d\Gamma - \overline{h}_\alpha \leqslant 0, \tag{15}$$

$$\int_{\Omega} \sigma : \mathbf{C} : \sigma_{\alpha} \, \mathrm{d}\Omega - (n-1) \int_{\Gamma_t} h_{\alpha}(\mathbf{u}_0) \, \mathrm{d}\Gamma - \overline{h}_{\alpha} \leqslant 0. \tag{16}$$

Each element in the design domain will be in one of following sets: set R_l where the design variables take the lower bound, set R_u where the design variables take the upper bound, and set R_a where the design variables take the active constraints. In the active constraint set, one has

$$\frac{\partial \rho}{\partial \mu} - \varphi_{\alpha} \mathbf{u} \nabla : \frac{\partial \mathbf{E}}{\partial \mu} : \mathbf{v}_{\alpha} \nabla = 0. \tag{17}$$

There are several ways to utilize Eq. (17) for updating the design variables. One way is to let [1,7]

$$\mu^{(k+1)} = \mu^{(k)} \left(\frac{\varphi_{\alpha} \mathbf{u} \nabla : \partial \mathbf{E} / \partial \mu : \mathbf{v}_{\alpha} \nabla}{\partial \rho / \partial \mu} \right)^{q} \equiv A, \tag{18}$$

where q is a weighting exponent, selected for an efficient iteration scheme. Another updating scheme [11] based on Eq. (17) is

$$\mu^{(k+1)} = \theta \mu^{(k)} + (1-\theta) \mu^{(k)} \left[\frac{\varphi_{\alpha} \mathbf{u} \nabla : \partial \mathbf{E} / \partial x : \mathbf{v}_{\alpha} \nabla}{\partial \rho / \partial x} \right] \equiv A. \tag{19}$$

Again another updating scheme is [8]

$$\mu^{(k+1)} = \mu^{(k)} - \left(\frac{\partial \rho}{\partial \mu} - \varphi_{\alpha} \mathbf{u} \nabla : \frac{\partial \mathbf{E}}{\partial \mu} : \mathbf{v}_{\alpha} \nabla \right) \equiv A. \tag{20}$$

Summing up the above discussion, one can update the design variable as follows:

$$\mu^{(k+1)} = \begin{cases} \mu_{\min} & \text{if } A \leqslant \mu_{\min} \\ A & \text{if } \mu_{\min} < A < \mu_{\max} \\ \mu_{\max} & \text{if } \mu_{\max} \leqslant A. \end{cases} \tag{21}$$

When complicated structures (like a material cell) is designed, one may instead use a moving limit δ, so that $\mu^{(k)}(1-\delta) \leqslant \mu^{(k+1)} \leqslant \mu^{(k)}(1+\delta)$.

To update the Lagrange multipliers φ_{α}, the following estimate

$$\int_{\Omega} \mathbf{u} \nabla : \mathbf{E} : \mathbf{v}_{\alpha} \nabla \, \mathrm{d}\Omega = \int_{\Omega} \sigma : \mathbf{C} : \sigma_{\alpha} \, \mathrm{d}\Omega \tag{22}$$

can be used in Eqs. (15) or (16). Non-linear equations for Lagrange multipliers φ_{α} can be solved by modified Newton–Stefensen iteration procedure. The modification concerns a careful treatment for the bounds of design variables.

In all examples shown in the sequel, the initial guess of the Newton–Stefensen procedure starts from $\varphi_{\alpha} = 1$. If the active constraints do not change, the Newton–Stefensen procedure should start from the value of φ_{α} arrived from the previous global iteration. If the active constraints change, it is advisable to start the Newton–Stefensen procedure from $\varphi_{\alpha} = 1$. Numerical experiences showed that the procedure converges within 10 iterations when start from $\varphi_{\alpha} = 1$. When start from the values of the last global iteration, only less than five iterations are required to converge.

The optimality criteria method is typically used in situations when the number of the global constraints is much less than the number of the design variables. Accordingly, the number of Lagrange multipliers is very small, and the cost for the procedure of computing Lagrange multipliers becomes negligible. Viewed from this perspective, the extra computational cost on the criteria optimality method procedure from a single constraint to the multiple constraints is rather minor. From the design variable updating procedure, we observed that the computer time for the updating procedure is virtually independent of the number of design variables. This feature gives the edge of the present method over various methods of non-linear mathematical programming. The computer time for the updating procedure of the latter, including the method of sequential linear programming, depends on the number of design variables, which is unfortunately very large in a topology design problem.

Topology optimization usually encounters checkerboard problem. In the following calculations, Sigmund's method [12] will be employed to overcome the checkerboard problem.

3. Structure design under multiple constraints

3.1. Multiple displacement constraints

Consider a short cantilever beam of in-plane dimension $80L \times 80L$ with multiple displacement constraints, as shown in Fig. 1a. Two upward point forces of intensity $P = 0.01E^0L$ are applied at the upper corner A and the lower corner B of the right side of the beam. The displacement constraints are

$$\begin{aligned} h_1 - \overline{h}_1 &= u_{A2} - \overline{h}_1 \leqslant 0, \\ h_2 - \overline{h}_2 &= u_{B2} - \overline{h}_2 \leqslant 0, \end{aligned} \tag{23}$$

where u_{A2}, u_{B2} are the vertical displacements of points A and B.

The domain is divided into 6400 elements. The following artificial material model is used:

$$E_{ijkl} = \rho^{\eta} E^0_{ijkl}, \quad \eta > 1, \tag{24}$$

where E^0_{ijkl} represents the material properties of an isotropic material with Young's modulus E^0 and Poisson's

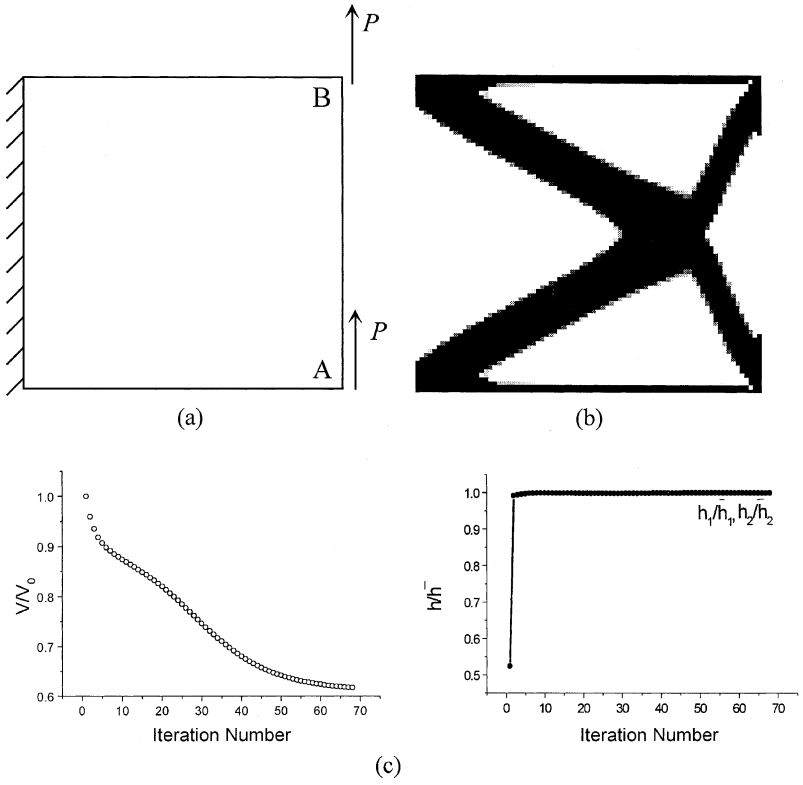

Fig. 1. (a) Definition of design domain. (b) Optimal design of $\overline{h}_1 = \overline{h}_2$. (c) Evolution of objective function and the constraints.

ratio $v = 0.3$. The penalizing factor is taken as $\eta = 2$, the bounds of design variables are taken as $\rho_{\max} = 1$ and $\rho_{\min} = 1 \times 10^{-4}$. Initial density is assigned to 0.7 for all elements. Fig. 1b shows the computed result under the given displacements $\overline{h}_1 = \overline{h}_2 = 0.4L$ and the weighting factor $q = 0.1$. Fig. 1c shows the evolution of objective and constraint functions, where the optimizing material volume V is normalized by the material volume of the initial design V_0.

3.2. Inactive displacement constraint

Next consider the case of inactive displacement constraint via a crack reinforcement problem shown in Fig. 2a. Three collinear cracks transverse the central line of a plate and subject to uniform remote tension. The middle crack locates at the plate center, and has a length of $10L$. The centers of the two side cracks are $16L$ on the left and the right from the plate center, and they have a longer length of $16L$. Symmetry dictates that one only needs to design the upper half of the plate. The selected design domain has a dimension of $80L \times 40L$. The objective is to find the optimal reinforcement distribution so that the maximum opening of three cracks is less than a given value, taken as $\overline{h}_1 = \overline{h}_2 = \overline{h}_3 = 0.25L$. A two-phase artificial-material model is used:

$$E_{ijkl} = \rho^{\eta} E^{(1)}_{ijkl} + (1 - \rho^{\eta}) E^{(2)}_{ijkl}, \quad \eta > 1. \tag{25}$$

Phase 1 refers to the strong reinforcement that has a stiffness tensor $E^{(1)}_{ijkl}$, and phase 2 refers to the weak matrix that has a stiffness tensor $E^{(2)}_{ijkl}$. Both are regarded as isotropic with their Young's moduli related by $E^{(1)} = 5E^{(2)}$ and Poisson's ratios $v^{(1)} = 0.3$ and $v^{(2)} = 0.2$. The parameters in the calculation are adopted as follows: the penalizing factor $\eta = 6$, the weighting factor $q = 0.3$, $\rho_{\max} = 1$ and $\rho_{\min} = 0$. Initial density is assigned to 0.9 for all elements.

The optimal reinforcement is shown in Fig. 2b. Dark gray color denotes strong reinforcement, while the light gray color denotes the matrix. The evolution of the objective and constraint functions is shown in Fig. 2c. The latter gives a clear indication that the second displacement constraint is inactive.

4. Design of elastic material

4.1. Formulation

The works of Sigmund [13], Sigmund and Gibiansky [14], Silva et al. [15] and Neves et al. [16] promote the

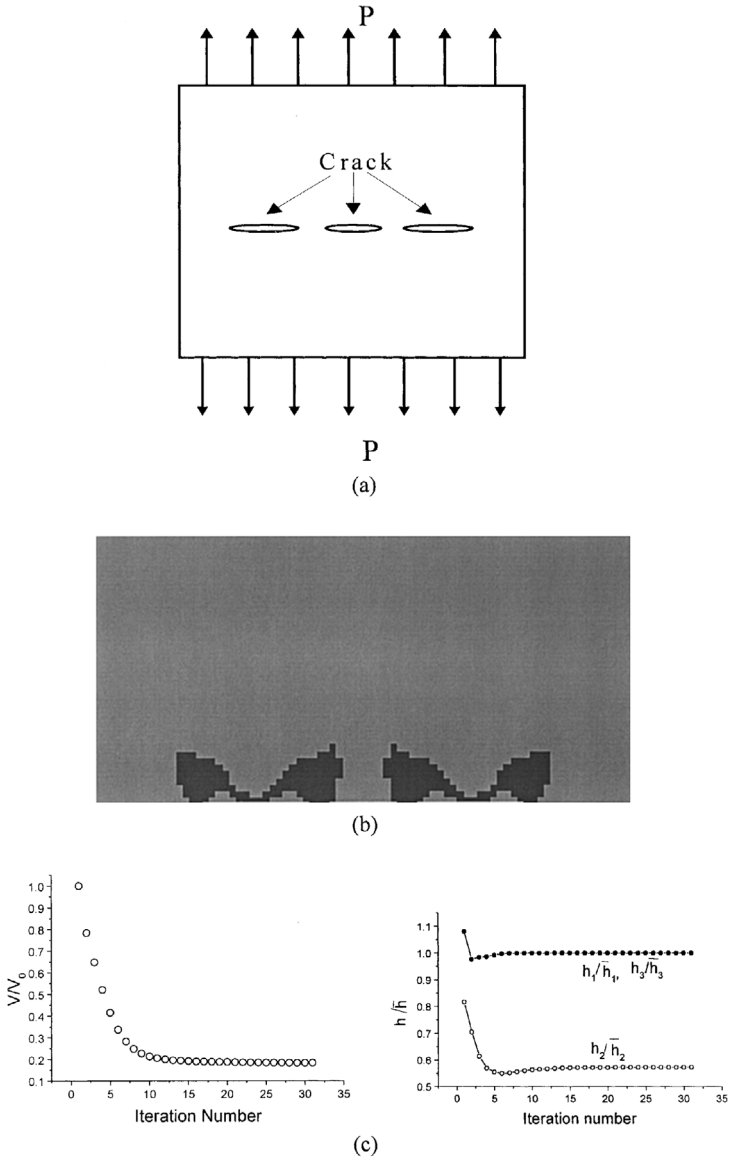

Fig. 2. (a) Three collinear cracks. (b) Optimal reinforcement to prevent crack opening, three shallow flutes denote the three cracks. (c) Evolution of objective function and three displacement constraints, the second is inactive.

investigation on topology optimization design of material cells. The early work of Sigmund [13] employed the optimality criteria method. His subsequent works on continuum-type problems, however, addressed the difficulty on using optimality criteria method to reach satisfying results. We will show that the framework of Section 2 gives the remedy to this difficulty.

For a structure consisting of periodic cells, the overall elastic tensor is given by [17]:

$$E_{ijkl} = \frac{1}{A}\int_A \left\{ E^{\xi}_{ijkl}(\xi) + E^{\xi}_{ijpq}(\xi)\frac{\partial \chi^{kl}_p}{\partial \xi_q} \right\} \mathrm{d}\xi, \tag{26}$$

where $\xi = (\xi_1, \xi_2)$ refers to the local coordinates for a representative cell. The equilibrium of microscopic field within the cell requires [16]

$$\left[E^{\xi}_{ijpq}(\xi)\left(\chi^{kl}_p + P^{kl}_p\right)_{,q} \right]_{,j} = 0, \tag{27}$$

where $P^{mn}_i = 1/2(\delta_{im}\xi_n + \delta_{in}\xi_m)$. An alternating form of Eq. (26) is cast in the following by using symbol P^{mn}_i

$$E_{ijkl} = \frac{1}{A}\int_A \left\{ E^{\xi}_{pqmn}(\xi)\left(\chi^{ij}_p + P^{ij}_p\right)_{,q}\left(\chi^{kl}_m + P^{kl}_m\right)_{,n} \right\} \mathrm{d}\xi. \tag{28}$$

The microscopic displacement $\boldsymbol{\chi}^{kl}$ is symmetric with respect to indices k and l, since it is caused by the strain tensor ε_{kl}. For a plane problem, only three independent displacement fields, $\boldsymbol{\chi}^{11}$, $\boldsymbol{\chi}^{22}$, $\boldsymbol{\chi}^{12}$ exist. Denote

$$\mathbf{w}^1 = \boldsymbol{\chi}^{11} + \mathbf{P}^{11}, \quad \mathbf{w}^2 = \boldsymbol{\chi}^{22} + \mathbf{P}^{22}, \quad \mathbf{w}^3 = \boldsymbol{\chi}^{12} + \mathbf{P}^{12}, \tag{29}$$

then Eq. (27) assembles a "Navier equation" for plane elasticity. The "displacement" $\mathbf{w}^\alpha$ is solved by

$$\left(E^{\xi}_{ijpq}(\xi) w^{\alpha}_{p,q}\right)_{,j} = 0, \quad \alpha = 1,2,3. \tag{30}$$

The boundary condition should be changed accordingly. For a cell symmetric with respect to ξ_1 and ξ_2 axes, one may combine the "displacement" definition (29) and the work of Hassani [18] to obtain the boundary conditions for $\mathbf{w}^\alpha$, as shown in Fig. 3. Suppose the cell has a dimension of $a \times b$. The Hassani boundary conditions are $w^1_1 = a$ along the right side for $\mathbf{w}^1$; $w^2_2 = b$ along the top side for $\mathbf{w}^2$; and $w^3_2 = (1/2)a$ along the right side and $w^3_2 = (1/2)b$ along the top side for $\mathbf{w}^3$.

The integral form of equilibrium equation (30) can be written as

$$\int_A E^{\xi}_{ijpq}(\xi) w^{\alpha}_{p,q} v^{\alpha}_{i,j} \,\mathrm{d}\xi - \int_{\Gamma_w} v^{\alpha}_i E^{\xi}_{ijpq}(\xi) w^{\alpha}_{p,q} n_j \,\mathrm{d}\Gamma = 0. \tag{31}$$

Substituting Eq. (29) into Eq. (28), one has

$$\overline{E}_{\alpha\beta} = \frac{1}{A}\int_A E^{\xi}_{pqmn}(\xi) w^{\alpha}_{p,q} w^{\beta}_{m,n} \,\mathrm{d}\xi, \tag{32}$$

where $\overline{E}_{\alpha\beta}$ is the imposed overall elasticity matrix for a plane strain problem.

For a cell symmetric with respect to ξ_1 and ξ_2, $\overline{E}_{11}$, $\overline{E}_{22}$, $\overline{E}_{12}$ and $\overline{E}_{33}$ are the only non-zero components of $\overline{E}_{\alpha\beta}$. The cell design aims at

$$\min \int_A \rho \,\mathrm{d}\xi \tag{33}$$

subjected to

$$\frac{1}{A}\int_A E^{\xi}_{ijkl} w^{\alpha}_{i,j} w^{\beta}_{k,l} \,\mathrm{d}\xi = \overline{E}_{\alpha\beta}, \quad \alpha,\beta = 1,2,3. \tag{34}$$

The remaining constraints are the equilibrium equation (30), and the bounds for material density ρ.

4.2. Updating schemes

For the optimization problem consisting of Eqs. (31), (33) and (34), it is straightforward to get the following optimality criteria for an intermediate density $\rho_{\min} < \rho < \rho_{\max}$,

$$\frac{\Lambda_{\alpha\beta}}{A}\frac{\partial E^{\xi}_{ijkl}}{\partial \rho} w^{\alpha}_{i,j} w^{\beta}_{k,l} = 1, \tag{35}$$

where $\Lambda_{\alpha\beta}$ are the Lagrange multipliers for the constraints (35). Eqs. (34) and (35) may be discretized as follows,

$$\sum_{\alpha,\beta=1}^{3} \Lambda_{\alpha\beta} P^{\alpha\beta}_e = 1, \tag{36}$$

$$\sum_e Q^{\alpha\beta}_e = \overline{E}_{\alpha\beta}, \quad \alpha,\beta = 1,2,3, \tag{37}$$

where e denotes the element number, A_e the domain occupied by the element,

$$P^{\alpha\beta}_e \equiv \frac{1}{A}\int_{A^e} \frac{\partial E^{\xi}_{ijkl}}{\partial \rho} w^{\alpha}_{i,j} w^{\beta}_{k,l} \,\mathrm{d}A \quad \text{and}$$

$$Q^{\alpha\beta}_e \equiv \frac{1}{A}\int_{A^e} E^{\xi}_{ijkl} w^{\alpha}_{i,j} w^{\beta}_{k,l} \,\mathrm{d}A.$$

Eqs. (36) and (37) are solved in two steps. When the design is far away from the optimal value, one may use the updating scheme (19) combined with the moving limit. That is

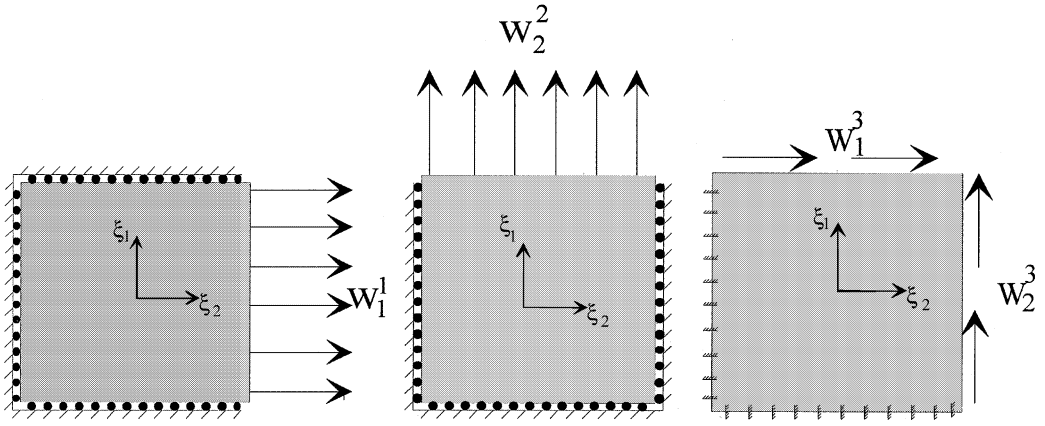

Fig. 3. Definitions of displacements $\mathbf{w}^1$, $\mathbf{w}^2$ and $\mathbf{w}^3$.

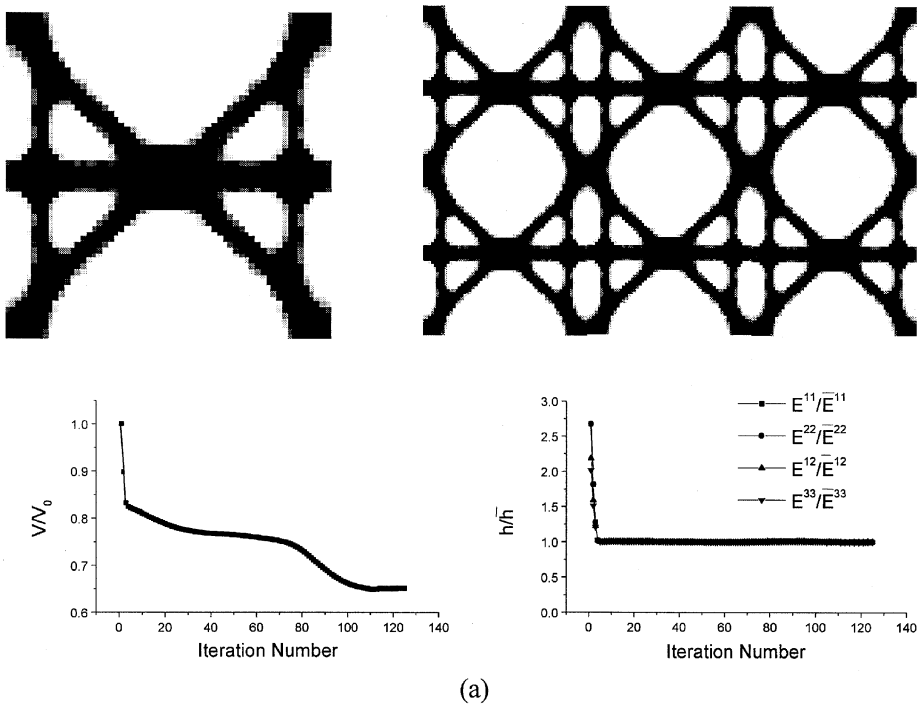

Fig. 4. Four cells with a Poisson's ratio of 0.3, their repetition and convergence: (a) first cell with a material volume of 0.377A; (b) second cell with a material volume of 0.368A; (c) third cell with a material volume of 0.375A; (d) fourth cell with a material volume of 0.367A.

$$\rho^{(k+1)} = \theta\rho^{(k)} + (1-\theta)\rho^{(k)}\left[\sum_{\alpha,\beta=1}^{3} \Lambda_{\alpha\beta} P_e^{\alpha\beta}\right]. \tag{38}$$

The adjustable parameter θ will take a value of 0.3 in the subsequent calculations. The linearization of Eq. (38)

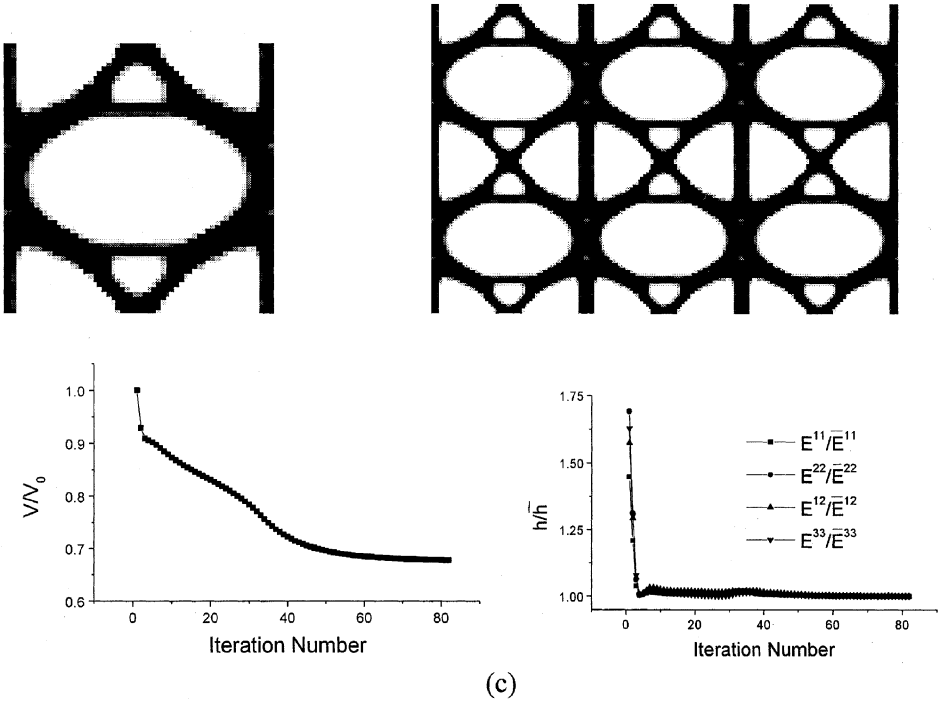

(c)

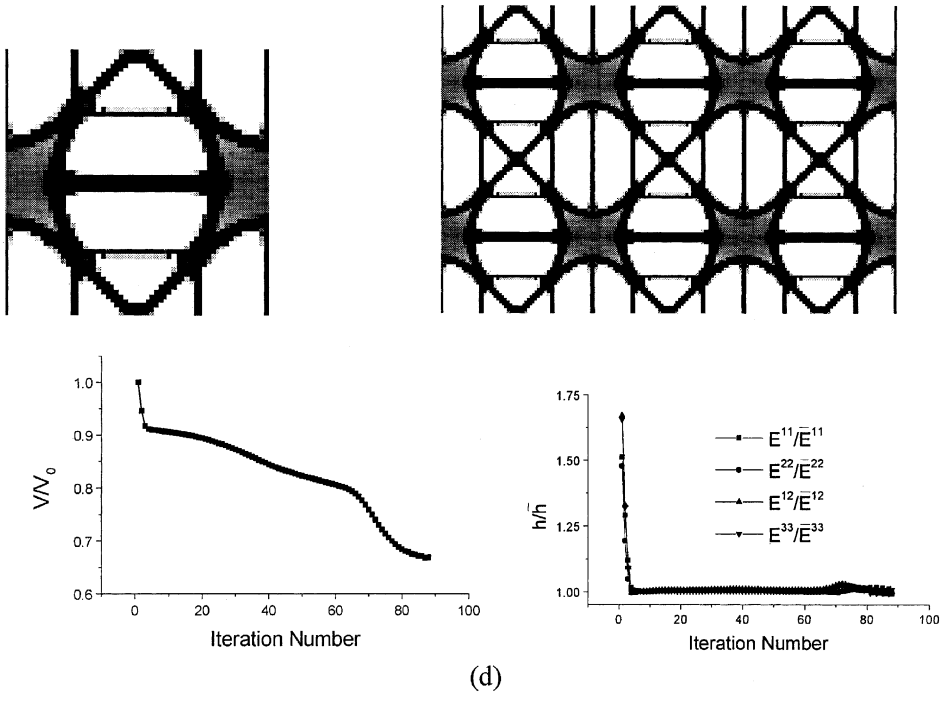

(d)

Fig. 4 (*continued*)

gives rise to an updating scheme for the Lagrangian multipliers. This can be accomplished by taking Taylor series expansion for the constraints (37),

$$\sum_e Q_e^{\alpha\beta}\left(\rho^{(k+1)}\right) = E^{\alpha\beta}(\rho^{(k)}) + \sum_e P_e^{\alpha\beta}\left(\rho^{(k)}\right)(\rho^{(k+1)} - \rho^{(k)}) = \overline{E}_{\alpha\beta}, \quad \alpha,\beta = 1,2,3. \tag{39}$$

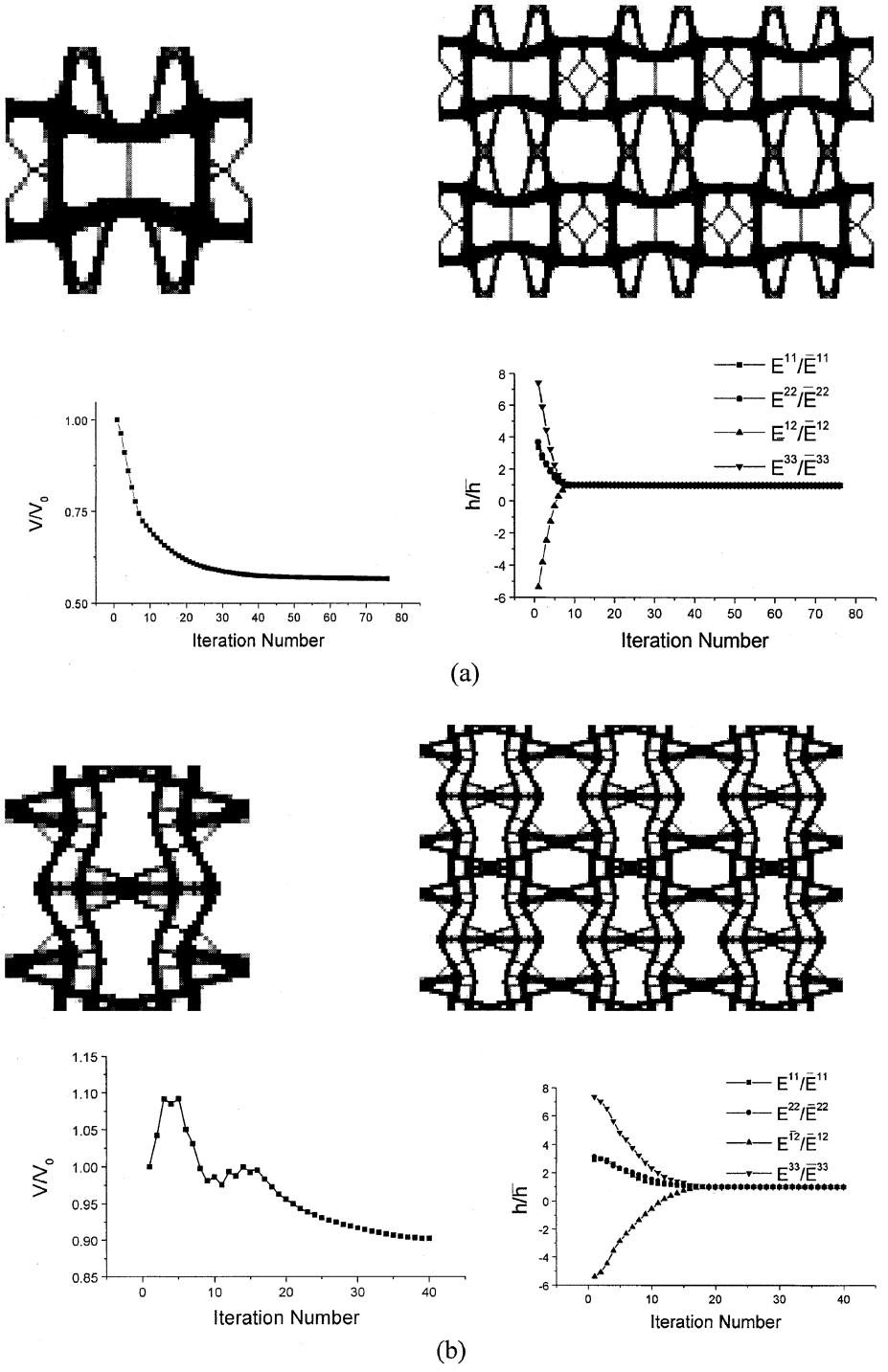

Fig. 5. Three cells with a Poisson's ratio of −0.23, their repetition and convergence: (a) first cell with a material volume of 0.365A; (b) second cell with a material volume of 0.386A; (c) third cell with a material volume of 0.385A.

When the design is converged to the vicinity of the optimal solution, the updating scheme is switched to:

$$\rho_{k+1} = \rho_k \left(\sum_{\alpha,\beta=1}^{3} \Lambda_{\alpha\beta} P_e^{\alpha\beta} \right)^q \tag{40}$$

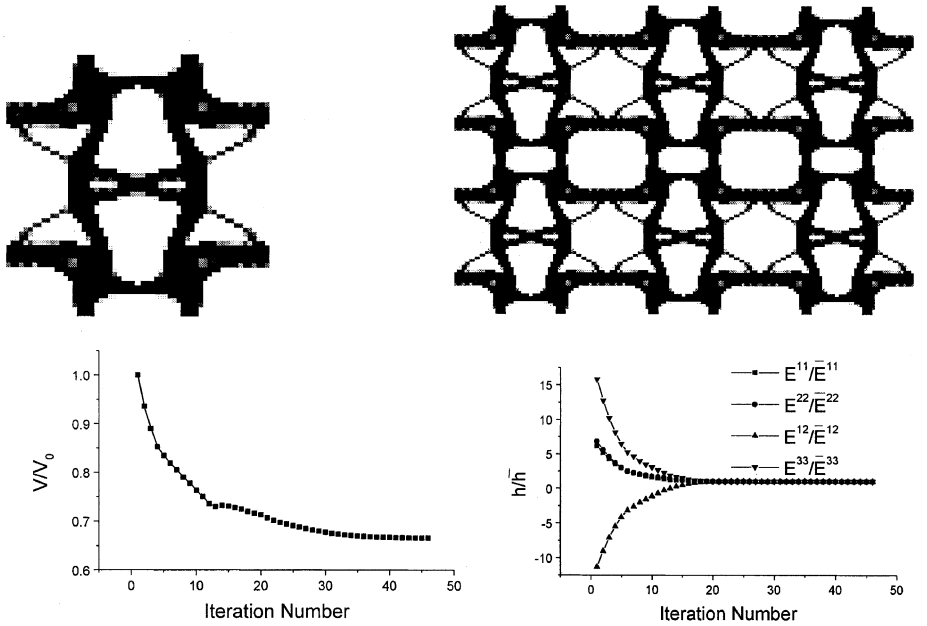

(c)

Fig. 5 (*continued*)

and the Langrange multipliers are updated by

$$\sum_e Q_e^{\alpha\beta}(\rho_{k+1}) = \overline{E}_{\alpha\beta}, \quad \alpha,\beta = 1,2,3. \tag{41}$$

That scheme accurately enforces the constraints during each iteration step.

4.3. Material of positive Poisson's ratios

In the examples to follow, the material is interpolated as $E_{ijkl}^{\xi} = \rho^2 E_{ijkl}^0$, where the matrix elastic tensor E_{ijkl}^0 is assumed to be isotropic with Young's modulus E and Poisson's ratio 0.3. The material cell is designed to have the following overall stiffness:

$$\begin{bmatrix} \overline{E}_{11} & \overline{E}_{12} & \overline{E}_{13} \\ \overline{E}_{21} & \overline{E}_{22} & \overline{E}_{23} \\ \overline{E}_{31} & \overline{E}_{32} & \overline{E}_{33} \end{bmatrix} = E \begin{bmatrix} 0.19 & 0.07 & 0 \\ 0.07 & 0.19 & 0 \\ 0 & 0 & 0.05 \end{bmatrix}. \tag{42}$$

In the structure optimization problems as exemplified in Sections 3.1 and 3.2, initial guess usually employs the uniform distribution density to avoid the local minima. However, the uniform distribution density cannot be employed in a material cell problem. It will lead to the uniform distribution of energy gradient that makes the next iteration impossible. When a structure consisting of periodic cell is of concern, one may get numerous cell topologies all sharing the same overall elasticity. Accordingly, the design of a material cell under prescribed elasticity would encounter numerous topologies. Here, four initial guesses are attempted and they converge to four different structures. Four optimal cell structures have nearly identical material volumes. One can further select the final design from those four cells from other considerations. In all graphs of Fig. 4, the top left figures are the designed cell, and the top right figures are formed by the cell repetition. The bottom figures show the convergence of the optimization process.

4.4. Material of negative Poisson's ratios

Attention is then focused on the design of material cells that lead to negative Poisson's ratios. Two examples are explored. The first design attempts the following overall elastic matrix and corresponds a Poisson's ratio of -0.23:

$$\begin{bmatrix} \overline{E}_{11} & \overline{E}_{12} & \overline{E}_{13} \\ \overline{E}_{21} & \overline{E}_{22} & \overline{E}_{23} \\ \overline{E}_{31} & \overline{E}_{32} & \overline{E}_{33} \end{bmatrix} = E \begin{bmatrix} 0.13 & -0.03 & 0 \\ -0.03 & 0.13 & 0 \\ 0 & 0 & 0.015 \end{bmatrix}. \tag{43}$$

Three types of designed cells are shown in Fig. 5.

The second design attempts the following overall elastic matrix and corresponds a Poisson's ratio of -0.54:

$$\begin{bmatrix} \overline{E}_{11} & \overline{E}_{12} & \overline{E}_{13} \\ \overline{E}_{21} & \overline{E}_{22} & \overline{E}_{23} \\ \overline{E}_{31} & \overline{E}_{32} & \overline{E}_{33} \end{bmatrix} = E \begin{bmatrix} 0.13 & -0.07 & 0 \\ -0.07 & 0.13 & 0 \\ 0 & 0 & 0.015 \end{bmatrix}. \tag{44}$$

Two designs emerge in Fig. 6, along with the convergence of the material volume and the constraints. Figs. 5 and 6

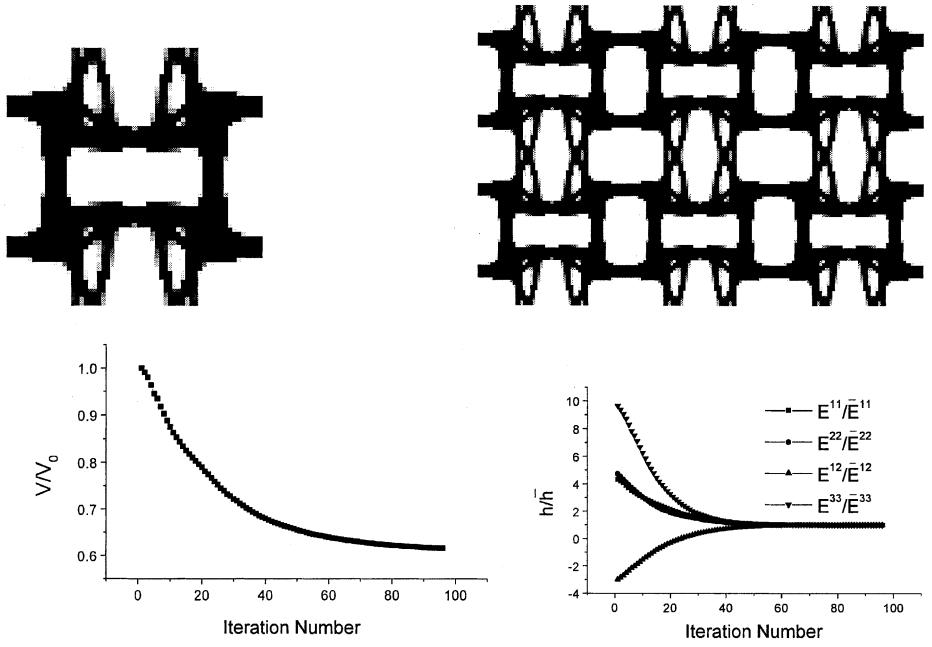

Fig. 6. Cell structure with a Poisson's ratio of −0.54, its repetition and convergence. The material volume is 0.427*A*.

identified two mechanisms to form a material with a negative Poisson's ratio. One mechanism involves the unfolding of curled segments within the cell when stressed, as evident in Fig. 5b and c. The other mechanism concerns the bending of zigzag segments under traction, as shown in Fig. 6. Two mechanisms co-exist in Fig. 5a.

5. Conclusions

1. We revise the optimality criteria method to accommodate multiple constraints. The gradient-split Taylor series expansion is employed to present the relationship between constraints and design variables in an explicit form. The computational cost for updating the Lagrangian multipliers is proved to be rather minor when the number of displacement constraints is small. The computational burden mainly comes from the analyses of various adjoint structures.

2. The power of the method is illustrated in several applications concerning the optimal designs of structures and materials. The issue of multiple displacement constraints and inactive constraint are explored. The design for material cells with negative Poisson's ratio reveals two mechanisms: unfolding of curled segments and the bending of zigzag segments.

Acknowledgements

The authors would like to thank for the support by National Natural Science Foundation of China.

References

[1] Bendsoe MP, Kikuchi N. Generating optimal topologies in structural design using a homogenization method. Comput Meth Appl Mech Engng 1988;71:197–224.
[2] Sigmund O, Torquato S. Design of materials with extreme thermal expansion using a three-phase topology optimization method. J Mech Phys Solids 1997;45(6):1037–67.
[3] Hassani B, Hinton E. A review of homogenization and topology optimization III: topology optimization using optimality criteria. Comput Struct 1998;69:739–56.
[4] Saxena A, Ananthasuresh GK. On an optimal property of compliant topologies. Struct Multidiscip O 2000;19:36–49.
[5] Diaz AR, Bendsoe MP. Shape optimization of multipurpose structures by a homogenization method. Struct Optim 1992;4:17–22.
[6] Mlejnek HK, Schirrmacher R. An engineer's approach to optimal material distribution and shape finding. Comput Meth Appl Mech Engng 1993;106:1–26.
[7] Yin LZ, Yang W. Topology optimization for tunnel support in layered geological structures. Int J Numer Meth Engng 2000;47:1983–96.
[8] Yin LZ, Ananthasuresh GK. Topology optimization of compliant mechanisms with multiple materials using a peak function material interpolation scheme. Struct Multidiscip Optimiz 2001;22(4):in press.
[10] Rozvany GIN, Zhou M. Optimality criteria methods for large discretized systems. In: Adeli H, editor. Advances in design optimization. London: Chapman & Hall; 1994. p. 42–108.
[11] Zhu B, Qi Z, et al. In: Principle and applications of structural optimization. Beijing: Waterpower Publisher; 1984. p. 80 [in Chinese].

[12] Sigmund O. On the design of compliant mechanisms using topology optimization. Mech Struct Mach 1997;25: 493–524.
[13] Sigmund O. Materials with prescribed constitutive parameters: an inverse homogenization problem. Int J Solids Struct 1994;31(17):2313–29.
[14] Gibiansky LV, Sigmund O. Multiphase composites with extremal bulk modulus. J Mech Phys Solids 2000;48(3): 461–98.
[15] Silva ECN, Fonseca JSO, de Espinosa FM, et al. Design of piezocomposite materials and piezoelectric transducers using topology optimization—Part I. Arch Comput Meth E 1999;6(2):117–82.
[16] Neves MM, Rodrigues H, Guedes JM. Optimal design of periodic linear elastic microstructures. Comput Struct 2000;76(1–3):421–9.
[17] Sanchez-Palencia E, Zaoui A. Homogenization techniques for composite media Lecture notes in physics, vol 272. Berlin: Springer; 1987.
[18] Hassani B. A direct method to derive the boundary conditions of the homogenization equation for symmetric cells. Commun Numer Meth Engng 1996;12:185–96.